Physics Letters B 832 (2022) 137252

Contents lists available at ScienceDirect

Physics Letters B

www.elsevier.com/locate/physletb

Binding-energy asymmetry in absorption explored through CDCC extended for complex potentials

M. Gómez-Ramos [a,*], J. Gómez-Camacho [a,b], A.M. Moro [a,c]

[a] Departamento de Física Atómica, Molecular y Nuclear, Facultad de Física, Universidad de Sevilla, Apartado 1065, E-41080 Sevilla, Spain
[b] Centro Nacional de Aceleradores (U. Sevilla, J. Andalucía, CSIC), Tomás Alva Edison, 7, 41092 Sevilla, Spain
[c] Instituto Interuniversitario Carlos I de Física Teórica y Computacional (iC1), Apdo. 1065, E-41080 Sevilla, Spain

ARTICLE INFO

Article history:
Received 3 March 2022
Received in revised form 24 May 2022
Accepted 2 June 2022
Available online 14 June 2022
Editor: J.-P. Blaizot

Keywords:
Continuum-discretized coupled channels
Optical model
Direct reactions
Three-body model

ABSTRACT

In this work, we present an extension of the Continuum-Discretized Coupled-Channel formalism to include the effects of absorption and excitation of the core through its interaction with the removed particle in the description of nuclear breakup reactions. This extension is performed via the inclusion of a complex energy-dependent interaction between core and removed particle and the use of a binormal basis to ensure orthogonality. The formalism is applied to neutron breakup reactions with a ^{12}C target at 70 MeV per nucleon for the loosely-bound ^{11}Be nucleus and the more deeply-bound ^{41}Ca nucleus, finding a moderate reduction in the cross section for the weakly-bound case and a strong reduction for the more deeply-bound case. Possible implications for the interpretation of intermediate-energy knockout reactions are discussed.

1. Introduction

Nucleon-removal reactions have a long and successful history in the study of the single-particle properties of nuclei [1–4]. In particular, nuclear breakup (or elastic breakup) reactions have been used extensively, specially in the study of loosely-bound and halo nuclei [5–9]. In these breakup reactions, a nucleon is removed from a nucleus a via interaction with a target A, leaving the target A in its ground state, as well as a residual core b and nucleon x ($a = b + x$), all of them detected in what is called the elastic breakup channel. The usual description for these reactions relies in a single-particle model of the nucleus, where the interaction between core b and removed nucleon x is assumed to be well described by an effective real interaction V_{bx} which reproduces the properties of the bound system a and in some cases the low-energy continuum of the $b-x$ system. The eigenstates of this potential are then taken as a good description of the continuum of the $b-x$ system and are used as the basis for Distorted Wave Born Approximation (DWBA) [10] or Continuum-Discretized Coupled-Channel (CDCC) [11] calculations to describe the reaction observables. However, in breakup reactions core b and nucleon x may end up in states with significant relative energies, where new channels beyond the single-particle excitation open, in particular the excitation and possible disintegration of b. The mere interaction between b and x can populate these open channels, thus reducing the cross section to the elastic breakup channel. These open channels cannot be considered in the description of breakup reactions described above but can nevertheless play a significant role, as has been shown for the breakup of ^{11}Be [12,13]. Generally the exclusion of these non-elastic channels restricts the description of breakup observables to low relative energies between the two fragments and to low binding energies of the removed nucleon, where their effect can be neglected. The exclusion of these open channels is particularly questionable when removing deeply-bound nucleons, where the large energy transfer enhances their population and subsequent decay of core nucleus b [14]. It is particularly in the removal of deeply-bound nucleons where a current open problem exists, in which theoretical predictions of nucleon-knockout cross sections severely overestimate experimental data [2,15], while for weakly-bound nucleons, the agreement is much better. We therefore find timely to explore the effects of non-elastic channels in breakup reactions, which will be included through the use of an effective complex energy-dependent interaction, in an approach similar to the widely-used optical model [10] and to the Ichimura-Austern-Vincent (IAV) description of non-elastic breakup [16]. It should be remarked that in Faddeev/AGS [17,18] calculations, the effects of complex potentials have been explored [19] but to our knowledge this study has not been extended to CDCC nor has it delved into the effects of non-orthogonality which naturally appear when considering complex potentials. The approach considered in this work

* Corresponding author.
E-mail address: mgomez40@us.es (M. Gómez-Ramos).

https://doi.org/10.1016/j.physletb.2022.137252

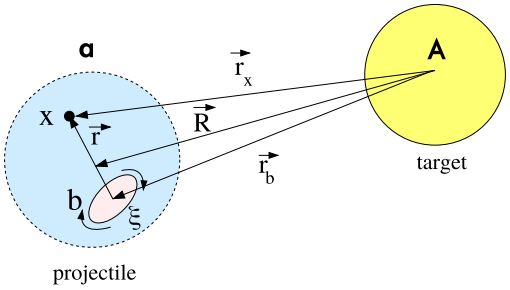

Fig. 1. Relevant coordinates for the description of the $A(a,bx)A$ reaction.

also opens CDCC to the use of state-of-the-art microscopic optical potentials [20–22], which are generally complex, non-local and energy-dependent, though their study will be left for a later publication.

This work is structured as follows: in Section 2 the formalism for CDCC with complex potentials is presented. In Section 3, results are presented for the ^{12}C(^{11}Be,^{10}Be$+n$)^{12}C and ^{12}C(^{41}Ca,^{40}Ca$+n$)^{12}C reactions. Finally, in Section 4, the results of this work are summarized and prospective lines of investigation are presented.

2. Theoretical framework

2.1. Effective three-body Hamiltonian

We start our derivation with the following Hamiltonian (see Fig. 1 for the relevant coordinates):

$$H = T_R + T_r + H_b(\xi) + V_{bx}(\mathbf{r},\xi) + U_{xA}(\mathbf{r}_x) + U_{bA}(\mathbf{r}_b), \tag{1}$$

where $H_b(\xi)$ is the core Hamiltonian, which depends explicitly on the core degrees of freedom ξ which couple strongly to those of the valence particle through V_{bx}. Its eigenstates will be denoted $\phi_b^{(c)}(\xi)$ (with $c=0$ denoting the ground state). The interactions U_{xA} and U_{bA} are assumed to be complex, as in standard in CDCC calculations, and represented by some optical potentials describing the respective fragment-target elastic scattering. By contrast, the potential $V_{bx}(\mathbf{r},\xi)$ is assumed to be real and depending on the considered core degrees of freedom (the x particle is assumed to be structureless for simplicity). Note that the use of complex U_{xA} and U_{bA} interactions assumes that a projection on the target ground state has been performed and hence the target internal coordinates do not appear explicitly in the Hamiltonian above. The complex interaction U_{bA} implicitly takes into account the excitation of the core b. However, the relevant core degrees of freedom that come into play in the interaction with the target U_{bA} should not significantly interfere with the degrees of freedom ξ that are excited due to the interaction with the valence particle V_{bx}. Therefore, the interaction U_{bA} can be assumed to be independent of ξ. A similar approximation was taken in the IAV description of inelastic breakup [16].

The three-body scattering wavefunction consistent with the Hamiltonian (1) can be expressed in integral form as

$$\Xi^{(+)}(\xi,\mathbf{r},\mathbf{R}) = \chi_a\phi_a + G_{3B}V_{\rm prior}\chi_a\phi_a \tag{2}$$

where

$$G_{3B} = \frac{1}{E^+ - T_R - U_{xA} - U_{bA} - H_{bx}} \tag{3}$$

with $E^+ = E + i\epsilon$, $\epsilon\to 0$ (E being the center-of-mass energy of the three-body system). $V_{\rm prior} = U_{xA} + U_{bA} - U_{aA}$ is the transition potential in the prior representation of the matrix element, as considered, for example, in transfer and inelastic breakup [10,16], and ϕ_a is the projectile ground state wavefunction. The distorted wave χ_a is a solution of the (arbitrary) auxiliary potential U_{aA} and H_{bx} is the projectile Hamiltonian

$$H_{bx}(\xi,\mathbf{r}) = H_b(\xi) + T_r + V_{bx}(\xi,\mathbf{r}). \tag{4}$$

The three-body wavefunction (2) depends, in addition to the internal and relative coordinates $\mathbf{r}$ and $\mathbf{R}$, on the core degrees of freedom ξ. In the standard CDCC formulation, the effects of the excitations of core b are ignored. Practical solutions of this three-body problem with core degrees of freedom have been recently carried out in a generalized CDCC method which includes these core excited components explicitly in the adopted model space [23,24]. In the present work we adopt a different approach in which these core excited components are not treated explicitly, but embedded in the effective two-body interactions. In other words, we seek for an approximate solution of the projected wavefunction $\Psi^{(+)}(\mathbf{r},\mathbf{R}) \equiv \langle\phi_b^{(0)}|\Xi^{(+)}\rangle$. As we will see, the presence of these core excitations generates modifications in the effective Hamiltonian which render the choice of the V_{bx} interaction more complicated than usually assumed in practical implementations. To see this in an approximate way, we assume that, in the projected model space, the ground state is well described by the product wavefunction $\phi_a(\xi,\mathbf{r}) \simeq \varphi_0(\mathbf{r})\phi_b^{(0)}(\xi)$ (where $\varphi_0(\mathbf{r})$ describes the $b+x$ relative motion in the projectile ground state). With this choice, the projected three-body scattering wavefunction results

$$\begin{aligned}\Psi^{(+)}(\mathbf{R},\mathbf{r}) &= \langle\phi_b^{(0)}|(1+G_{3B}V_{\rm prior})|\chi_a\phi_b^{(0)}\varphi_0\rangle \\ &= \left[1 + \langle\phi_b^{(0)}|G_{3B}|\phi_b^{(0)}\rangle V_{\rm prior}\right]\chi_a\varphi_0 \\ &= \left[1 + \frac{1}{E^+ - T_R - U_{xA} - U_{bA} - T_r - U_{bx}}V_{\rm prior}\right]\chi_a\varphi_0\end{aligned} \tag{5}$$

where, in the last line, we have used the definition of the formal optical model Green's function:

$$G^{\rm opt}(z) = \langle\phi_b^{(0)}|\left[\frac{1}{z - H_{bx}}\right]|\phi_b^{(0)}\rangle = \frac{1}{z - T_r - U_{bx}} \tag{6}$$

where U_{bx} is the formal $b+x$ elastic scattering optical potential. The last line of equation (5) indicates that the formal elimination of the core degrees of freedom necessarily leads to an effective interaction (U_{bx}) which, in general, will be complex and energy dependent. Note that, even at excitation energies below the first b excited state, the U_{bx} interaction will contain polarization effects which induce deviations from the bare $b+x$ interaction [12,13].

2.2. CDCC equations in a binormal basis

It is therefore required to extend CDCC calculations to consider complex and energy-dependent potentials for the core-valence interaction. As a starting point, let us briefly re-derive the standard CDCC equations [11], starting from the Schrödinger equation:

$$(T_R + T_r + V_{bx} + U_{bA} + U_{xA} - E)\Psi(\mathbf{R},\mathbf{r}) = 0. \tag{7}$$

Now we introduce the CDCC expansion for the wavefunction of the system Ψ:

$$\begin{aligned}\Psi &= \sum_{b\gamma J^\pi}\chi_{b\gamma}^{J^\pi}(\mathbf{R})\varphi_{b\gamma}^{J^\pi}(\mathbf{r}) + \sum_{\gamma J^\pi}\int {\rm d}k\,\chi_\gamma^{J^\pi}(k,\mathbf{R})\varphi_\gamma^{J^\pi}(k,\mathbf{r}) \\ &\simeq \sum_{b\gamma J^\pi}\chi_{b\gamma}^{J^\pi}(\mathbf{R})\varphi_{b\gamma}^{J^\pi}(\mathbf{r}) + \sum_{n\gamma J^\pi}\chi_{n\gamma}^{J^\pi}(\mathbf{R})\varphi_{n\gamma}^{J^\pi}(\mathbf{r}) \equiv \sum_i \chi_i(\mathbf{R})\varphi_i(\mathbf{r}),\end{aligned} \tag{8}$$

where $\varphi^{J^\pi}_{b\gamma}(\mathbf{r})$ are the bound eigenstates of potential V_{bx} and $\varphi^{J^\pi}_{\gamma}(k,\mathbf{r})$ its eigenfunctions in the continuum as a function of k, the modulus of the relative momentum between b and x. Both sets of wavefunctions have a defined total angular momentum and parity J^π and $\gamma = \{(ls_x)jI_bM\}$, the other quantum numbers required to describe the spin-angular configuration (the orbital angular momentum l, the spin of x s_x, their sum j, the spin of b I_b and the total magnetic angular momentum M in this case). The continuum wave functions are approximated by a discrete set of functions $\varphi^{J^\pi}_{n\gamma}$ [11], built to be orthogonal. The following derivations do not distinguish between bound $\varphi^{J^\pi}_{b\gamma}(\mathbf{r})$ and discretized continuum states $\varphi^{J^\pi}_{n\gamma}$ so we will use index i to denote both bound and discretized continuum states. χ_i is the coefficient of state φ_i and depends on $\mathbf{R}$. As the wavefunctions are eigenvalues of the real potential V_{bx}, they are orthogonal so one can obtain a set of equations for χ_i by multiplying to the left by $\langle\varphi_i|$:

$$\sum_j \left((T_R - E_i)\langle\varphi_i|\varphi_j\rangle + \langle\varphi_i|U_{bA}+U_{xA}|\varphi_j\rangle\right)\chi_j(\mathbf{R}) =$$
$$\sum_j \left((T_R - E_i)\delta_{ij} + U_{ij}\right)\chi_j(\mathbf{R}) = 0, \tag{9}$$

where the bracket denotes integration over $\mathbf{r}$, and we have used $(T_r + V_{bx})\varphi_i(\mathbf{r}) = \epsilon_i\varphi_i(\mathbf{r})$ with $E_i = E - \epsilon_i$ and introduced the coupling potentials $U_{ij} = \langle\varphi_i|U_{bA}+U_{xA}|\varphi_j\rangle$.

In order to derive these expressions one fundamental assumption is the orthogonality of states φ_i and φ_j. However, if one were to consider a complex or energy-dependent potential, its eigenstates would no longer constitute an orthogonal basis, as is well known. However, even in this case it is possible to derive analogous expressions through the use of a binormal or biorthogonal basis $\tilde{\varphi}_i$, which is defined as [25]:

$$\langle\tilde{\varphi}_i|\varphi_j\rangle = \langle\varphi_i|\tilde{\varphi}_j\rangle = \delta_{ij}. \tag{10}$$

In this case, one needs only to multiply Eq. (9) by $\langle\tilde{\varphi}_i|$ to obtain the set of equations for χ_j:

$$\sum_j \left((T_R - E_i)\delta_{ij} + \langle\tilde{\varphi}_i|\,U_{bA}+U_{xA}\,|\varphi_j\rangle\right)\chi_j(\mathbf{R}) = 0. \tag{11}$$

Therefore, one can solve the Schrödinger equation for a complex energy-dependent potential simply by modifying the coupling potentials $\tilde{U}_{ij} = \langle\tilde{\varphi}_i|\,U_{bA}+U_{xA}\,|\varphi_j\rangle$, which however requires the knowledge of $\tilde{\varphi}_i$, the binormal states to the eigenstates of the potential. To compute the binormal states, we use a procedure which is similar to the discretized version of the expressions by McKellar and McKay [26].

The states φ_i used in our CDCC calculations include the bound ground state φ_0, which is an eigenstate of the nucleon-core Hamiltonian with a real potential V_{bx}, plus a set of bins of continuum states $\varphi^{(-)}_i$ of the complex potential U_{bx} (V_{bx} and U_{bx} can be different since we allow for energy dependence). These bins are, as per usual, constructed from continuum states which are asymptotically given as a unit-amplitude outgoing wave plus incoming waves $\varphi^{(-)}_i \sim h^{(1)}_\ell(kr) - C_\ell h^{(2)}_\ell(kr)$, with $h^{(1)}$, $h^{(2)}$ being the outgoing and incoming Hankel functions. It is convenient to obtain $\varphi^{(-)}_i$ as the complex conjugate of the solution $\varphi'^{(+)}_i$ of the conjugate potential U^*_{bx}, which verifies $\varphi'^{(+)}_i \sim h^{(2)}_\ell(kr) - S'_\ell h^{(1)}_\ell(kr)$, with unit-amplitude incoming wave plus outgoing waves [10].

In order to obtain the binormal states $\tilde{\varphi}_i$ to the states φ_i described above, we start with the observation that, if the potentials were energy independent, the binormal states to $\varphi^{(-)}_i$ would precisely be the states $\varphi^{(+)*}_i$, the conjugates to the solutions of the same complex potential U_{bx}, but with unit-amplitude-incoming-wave boundary conditions [27]. This observation gives us a first approach for the binormal states.

$$\tilde{\varphi}^{(-)}_i \simeq \varphi^{(+)*}_i. \tag{12}$$

Calculations using this approximation will be labeled as "Complex non-orthogonal" or "Complex NO" in the following. Note that, in this approach, the binormal for the bound state would be the same bound state. Due to energy dependence, this approximation does not produce states that are strictly binormal. However, the states $\varphi^{(+)*}_i$ can be taken as a first approximation to the binormal states, which should be valid when the energy dependence of the potential is small. The approximation $\tilde{\varphi}^{(-)}_i \sim \varphi^{(+)*}_i$ also gives some insight on the effect of the complex potential in breakup reactions. In particular, for reactions at sufficiently high energies, the breakup process can be seen as one step from the bound state φ_0 to the continuum state φ_i, led by the coupling potential $U_{i0} = \langle\varphi_i|U_{bA}+U_{xA}|\varphi_0\rangle$ for a real U_{xb} interaction. The inclusion of an absorptive complex potential in U_{xb} results (within this approximation) in a coupling potential $\tilde{U}_{i0} \sim \left\langle\varphi^{(+)*}_i|U_{bA}+U_{xA}|\varphi_0\right\rangle$. Now, it is well known that the effects of absorption reduce the wavefunction in the nuclear interior, the region explored by U_{i0}, since φ_0 is bound. As such, one can expect $\left|\tilde{U}_{i0}\right| < |U_{i0}|$, resulting in a smaller cross section, which is the intuitive effect of absorption.

The proper calculation of the binormal states $\tilde{\varphi}_i$ to ensure orthogonality can be performed starting from the states $\varphi^{(+)*}_i$ and finding the adequate linear combination that fulfills:

$$\tilde{\varphi}^{(-)}_i = \sum_j \left(\mathcal{A}^{-1}\right)_{ji}\varphi^{(+)*}_j \tag{13}$$

$$\mathcal{A}_{ij} = \left\langle\varphi^{(-)}_i|\varphi^{(+)*}_j\right\rangle. \tag{14}$$

Note that states of different angular momentum and parity J^π are already orthogonal so the orthogonalization procedure only needs to consider bins with the same J^π. Trivially, when the potential is real and energy-independent $\varphi^{(-)}_i = \varphi^{(+)*}_i$ and $\left\langle\varphi^{(-)}_j|\varphi^{(-)}_i\right\rangle = \delta_{ij}$, so the binormal $\tilde{\varphi}^{(-)}_i$ is the same $\varphi^{(-)}_i$.

3. Results

We will first consider as a test case the breakup reaction ^{12}C(^{11}Be,n^{10}Be)^{12}C at 70 MeV per nucleon, for which experimental data exist [7]. For the real part of the interaction between neutron and ^{10}Be, we have considered the potential from Capel et al. [28]. There is unfortunately no data on low-energy reaction cross sections for the n+^{10}Be system. As such we have opted to fit the reaction cross sections taken from the compilation of [29] for p,n+^{9}Be, rescaled by a factor $(10/9)^{2/3}$ to account for the different sizes of the nuclei. It should be noted that for ^{9}Be non-elastic channels (in this case dissociation in $n+2\alpha$) already open at a relative energy between n and ^{9}Be of 1.6 MeV while for ^{10}Be the first non-elastic channel (excitation to the 2^+ level) opens at a relative energy between n and ^{10}Be, $E_{n^{10}\mathrm{Be}}$, of 3.4 MeV. As such, this procedure likely overestimates the imaginary potential for $E_{n^{10}\mathrm{Be}}$ in this range. For the imaginary part of the n+^{10}Be potential, we have considered the parametrization (for $E_{n^{10}\mathrm{Be}} > 0$):

$$W(E_{n^{10}\mathrm{Be}}, r) = -\frac{W_0(E_{n^{10}\mathrm{Be}})}{1+\exp(r-R)/a_0}$$
$$W_0(E_{n^{10}\mathrm{Be}}) = \frac{(a(E_{n^{10}\mathrm{Be}} - E_b)+b)E^4_{n^{10}\mathrm{Be}}}{E^4_{n^{10}\mathrm{Be}} + E^4_b}, \tag{15}$$

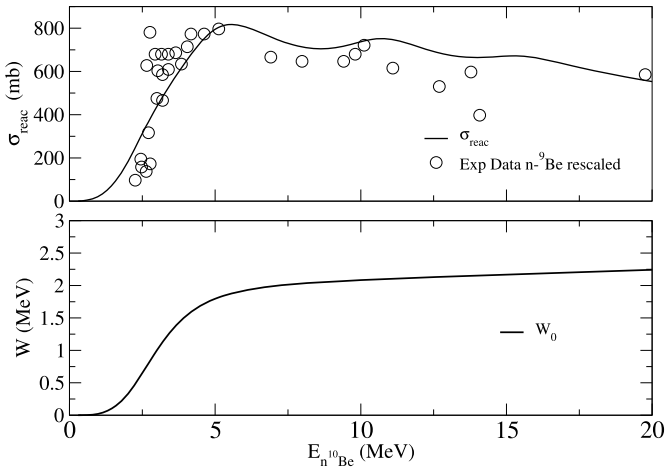

Fig. 2. n+^{10}Be reaction cross section computed with the parametrization considered in this work. Experimental data have been adapted from those in [29] (see text for details). The top panel shows the reaction cross section while the bottom panel shows the depth of the potential as a function of energy.

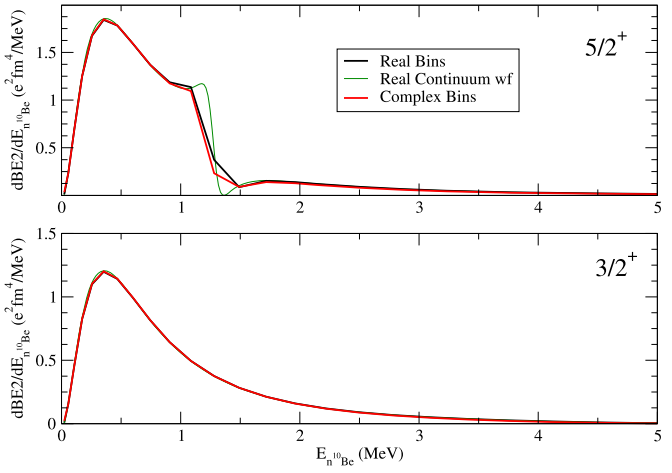

Fig. 3. Quadrupole electric transition probability for the nucleus ^{11}Be. The top and bottom panels correspond to $J^\pi = 5/2$ and $J^\pi = 3/2$, respectively. The red solid line corresponds to a calculation with a complex $U_{n^{10}\mathrm{Be}}$ potential and bins, the black solid line to a real $U_{n^{10}\mathrm{Be}}$ potential and bins and the green thin line to a real potential and exact continuum wavefunctions.

which presents the sharp increase seen in the data while being analytical. The results of the fit are shown in Fig. 2, where the top panel shows the reaction cross section and the bottom panel the depth of the potential, both as a function of $E_{n^{10}\mathrm{Be}}$. The parameters giving this fit are as follows: $R = 4.33$ fm, $a_0 = 0.8$ fm, $E_b = 3$ MeV, $a = 0.0143$ and $b = 2$ MeV. Despite the aforementioned overestimation of the imaginary potential, we consider this description of the n-^{10}Be interaction to be realistic enough for the purposes of this work.

With this parametrization of the interaction we are able to explore the continuum of ^{11}Be. The calculations were performed in general using 60 bins up to an energy of 30 MeV for each partial wave. States of negative energy except for the ground state have not been considered. We find results to be converged with this number of bins and verified the orthogonality between the bins and their binormal states, finding non-orthogonality in the norm which amounted to less than 10^{-8} between any pair of states. We first focus on the states with $L = 2$ between n and ^{10}Be. We present in Fig. 3 the $B(E2)$ quadrupole reduced transition probability for the $5/2^+$ and $3/2^+$ states as a function of $E_{n^{10}\mathrm{Be}}$. In the case of a complex energy-dependent potential the formula for the

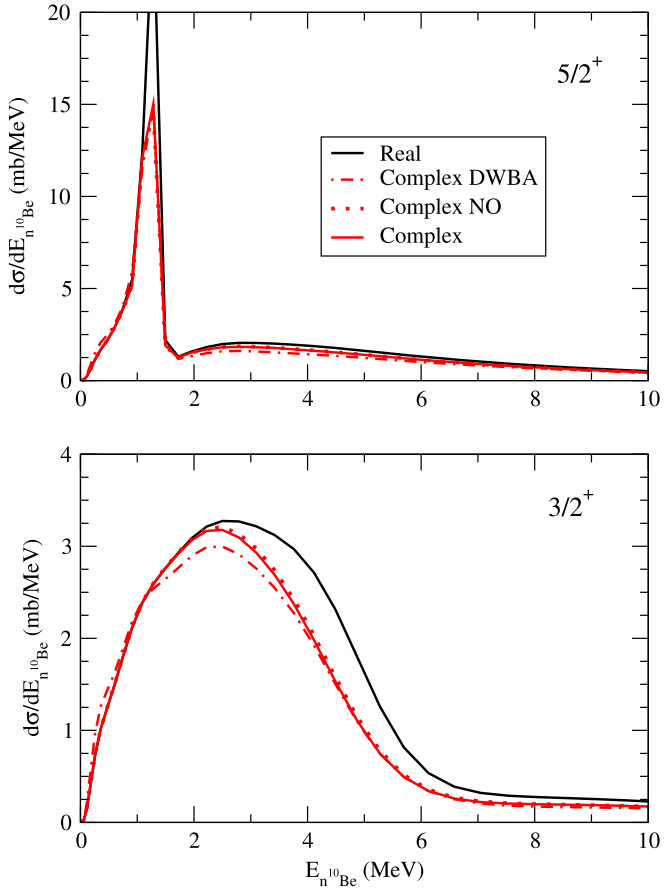

Fig. 4. Differential breakup cross section for the reaction ^{12}C(^{11}Be, n +^{10} Be)^{12}C at 70 MeV per nucleon. The top panel corresponds to final states with $J^\pi = 5/2^+$ and the bottom panel to states with $J^\pi = 3/2^+$. The red solid line corresponds to calculations with a complex $U_{n^{10}\mathrm{Be}}$ potential and the black solid line corresponds to a real $U_{n^{10}\mathrm{Be}}$ potential. The red dot-dashed line corresponds to DWBA calculations with the complex potential while the red dotted line corresponds to a full CDCC calculation using Eq. (12) (see text for details).

$B(E2)$ changes in the intuitive way: $B(E2) \propto |\langle\tilde{\varphi}_{\mathbf{k}}|\hat{O}(E2)|\varphi_{\mathrm{gs}}\rangle|^2$. In the figure we present the calculation of the $B(E2)$ with a real potential (the one presented with $W(r) = 0$) considering exact continuum wavefunctions in the green thin line and continuum bins in the black solid line. For the complex potential, we can only compute the binormal states for the bins. Hence only the results for bins are presented in the red solid line. In general, the results are very similar for real and complex potentials, as can be expected, since the imaginary part is very small for energies $E_{n^{10}\mathrm{Be}} < E_b$. Only for the narrow resonance we see a significant discrepancy between the results with bins and whose with exact continuum wavefunctions, due to the abruptness of the behavior of the $B(E2)$, which makes it difficult to describe with bins of reasonable width.

However, for the very narrow $5/2^+$ resonance we see a small dip when comparing the results with bins for real and complex potentials. This effect is enhanced when studying the cross section as a function of energy for the ^{12}C(^{11}Be, ^{10}Be+n)^{12}C reaction at 70 MeV/A, which is presented for the $5/2^+$ and $3/2^+$ states in Fig. 4.

The breakup cross section has been computed using the CDCC formalism, with similar inputs to those in [30], in particular the optical potentials: Between ^{10}Be and ^{12}C a folding potential with the CEG07 interaction [31] was considered, while between n and ^{12}C the Köning-Delaroche interaction (KD) [32] was used. In Fig. 4, the black and red solid lines correspond to real and complex potentials respectively. Here it can be seen that for $J^\pi = 5/2^+$ the effect of the complex interaction is strongest in the resonance,

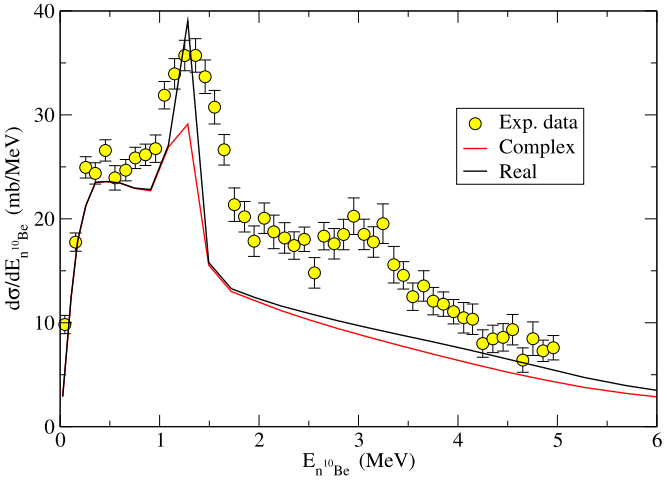

Fig. 5. Breakup cross section for the ^{12}C(^{11}Be, $n+^{10}$Be)^{12}C reaction at 70 MeV per nucleon as a function of $n-^{10}$Be energy. The solid red line corresponds to calculations with a complex $U_{n^{10}\mathrm{Be}}$ potential and the solid black line corresponds to a real $U_{n^{10}\mathrm{Be}}$ potential. Experimental data are taken from [7].

whose peak is reduced by a factor of 40%, while the tail above the resonance presents a reduction of $\sim 10\%$ and the overall cross section is reduced from 23.8 mb to 19.9 mb. For $j^\pi = 3/2^+$, the effect is quite more noticeable, with a clear reduction of the cross section starting around $E_b = 3$ MeV, reaching 40% at 5-6 MeV and slowly reducing to 20% at 10 MeV, with the cross section reduced from 16.1 mb to 13.7 mb.

The increased effect of the complex potential in the $5/2^+$ resonance can be understood, as a resonant state is enhanced in the nuclear interior, where the absorption due to the imaginary part of the potential is largest. This, in turn, also explains the reduced effect in the $B(E2)$, which is more sensitive to larger $n+^{10}$Be distances than the (mostly nuclear) ^{12}C(^{11}Be, ^{10}Be $+ n$)^{12}C reaction. The larger reduction found for the $3/2^+$ states has a similar explanation, as the $3/2^+$ continuum for this potential presents a broad resonant-like structure that spans the interval between 3 and 8 MeV and is thus more sensitive to absorption, although perhaps not to the extent of the narrow $5/2^+$ resonance. In fact, for the other partial waves considered (s and p waves), which do not present a resonant behavior, the effect of absorption is smaller, of less than 10%.

The effects of the complex potential on the cross section should not be understood only as a consequence of absorption for the final channel, as the orthogonalization of the continuum states and the more standard coupled channel effects can also play a role. In order to clarify their relevance in Fig. 4 two additional calculations are presented: In the red dot-dashed line, a DWBA calculation is performed to study the effects of coupled-channels, which are found to be minor in this case, with a 4-5% change in the total cross section, although in the $5/2^+$ case at $\sim$4 MeV the changes reach $\sim 10\%$.

The red dotted line in Fig. 4 corresponds to the complex non-orthogonal approximation where, instead of the binormal states $\tilde{\varphi}_i^{(-)}$, the functions $\varphi_i^{(+)*}$ were used. These states are not orthogonal and should formally not be used, as they introduce spurious contributions due to non-orthogonality. However, in this case they are found to give identical results to the binormal states, which can be related to the rather small energy dependence of the complex potential and the fact that the bound state does not correspond to these two waves.

As a final observable for this reaction, in Fig. 5 the full breakup cross section (including s-, p- and d-wave breakup, as in [33,34]) for $\theta_{cm} = 0 - 12^\circ$ is presented for the real (black solid line) and complex (red solid line) potential. Due to computational limitations the discretization of the continuum for each partial wave corresponds to 30 bins instead of 60. Experimental data from [7] are shown for reference. Although in this work we do not seek agreement with the experimental data, it is worth mentioning that this reaction was shown in [12] to have an important contribution from the dynamic excitation of the ^{10}Be core due to its interaction with the target. This contribution is not included in the present models. Therefore, the calculation with the real potential underestimates the data, and more so the one with the complex potential, which produces a smaller cross section due to the nucleon-core absorption. This disagreement could be improved through the explicit inclusion of core excitation in the reaction model together with a complex potential. This, however, is beyond the objectives of this work. For the full cross section, the effects of absorption follow the trend shown in the previous results, showing no effects for small energies except for the resonance, which is significantly reduced, and then a small reduction in the cross section appearing around $E \sim 2.5 - 3$ MeV and remaining for larger energies. The integrated cross sections are 80 mb for the real potential and 73 mb for the complex one, so the effect of the imaginary part of the potential amounts to a moderate reduction in cross section of $\sim 9\%$. The overestimation of the imaginary part of the $n-^{10}$Be interaction at low energies mentioned previously may produce too large a difference between the two calculations in the region of the resonance, so the reduction factor could be even smaller.

The modesty of the effects of the complex potential can be ascribed to three factors. Firstly, the strength of the imaginary potential is quite small. As seen in Fig. 2, it barely reaches 2 MeV for energies below 20 MeV. Secondly, the nucleus considered, ^{11}Be, is weakly bound and exhibits a halo structure so the breakup reaction explores large $n-^{10}$Be distances, where the effect of the imaginary potential is weaker. Thirdly, the breakup of a weakly-bound nucleus preferably populates states with smaller momentum and energy, where the lack of open channels which could absorb flux results in a smaller imaginary potential at these low energies, and thus in a smaller effect on the observables.

It is therefore interesting to explore a more deeply-bound nucleus, to assess how the effects of absorption between nucleon and core evolve with binding energy. We have therefore chosen to study the reaction ^{12}C(^{41}Ca, $n+^{40}$Ca)^{12}C at 70 MeV/A, which is analogous to the previous one save for the studied nucleus. For the optical potentials in this reaction, we have kept the KD interaction for neutron-^{12}C, and used the São Paulo interaction [35] with the standard normalization factors 1 and 0.78 for the real and imaginary parts of the ^{12}C-^{40}Ca interaction. For the interaction between neutron and ^{40}Ca we used the KD global potential, which reproduces the reaction cross section between neutron and ^{40}Ca for a wide range of energies as well as the binding energy of the valence neutron in ^{41}Ca, at which the interaction becomes real. The calculation considered for the continuum all partial waves with $L = 0 - 3$ between n and ^{40}Ca. Each partial wave was described with 25 bins up to a n-^{40}Ca relative energy ($E_{n^{40}\mathrm{Ca}}$) of 30 MeV. The ground state was the only negative-energy state considered, as other bound states are not reproduced by the KD interaction.

The cross section as a function of energy is presented in Fig. 6, where the red solid line corresponds to the full complex energy-dependent interaction between neutron and ^{40}Ca while the black solid line corresponds to the real energy-independent interaction, which is taken as the KD interaction at the (negative) neutron separation energy, thus producing the same bound state. As can be seen in the figure the effects of the complex interaction are in this case significantly larger, reducing the cross section by $\sim 50\%$. The distribution for the real energy-independent potential presents a resonant-like structure with $J^\pi = 5/2^+$ at $E_{n^{40}\mathrm{Ca}}$ $\sim$2 MeV and another very broad structure with $J^\pi = 7/2^-$ at $E_{n^{40}\mathrm{Ca}}$ $\sim$6-7 MeV,

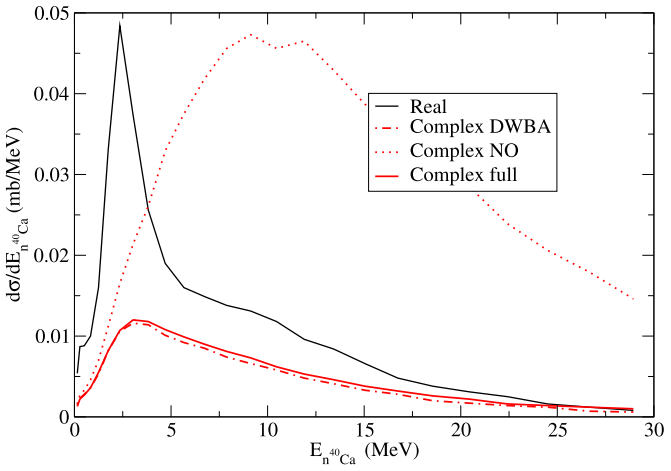

Fig. 6. Energy differential breakup cross section for the $^{12}C(^{41}Ca, n+^{40}Ca)^{12}C$ reaction at 70 MeV per nucleon as a function of the relative energy between n and ^{40}Ca. The solid red line corresponds to calculations with a complex $U_{n^{40}Ca}$ potential and the solid black line corresponds to a real $U_{n^{40}Ca}$ potential. The dot-dashed red line corresponds to a DWBA calculation with the complex potential while the dotted red line corresponds to the full CDCC calculation using Eq. (12) (see text for details).

both of which are significantly reduced by the complex energy-dependent potential. As in Fig. 4, we present in the red dot-dashed line the results of the DWBA calculation, finding also in this case that higher-order effects are minor, which can be expected, as the energy of the reaction is similar. However, we find a very strong effect when considering the complex non-orthogonal approximation (i.e., using $\varphi_i^{(+)*}$ instead of $\tilde{\varphi}_i^{(-)}$), producing a cross section that is much larger than even that for a real potential. Further exploration shows that the $7/2^-$ wave presents the largest effect for this calculation. This large spurious contribution originates in the non-orthogonality between the continuum states and the bound state (which has also $J^\pi = 7/2^-$). This shows that it is fundamental to ensure the orthogonality of states, specially for the partial wave associated to the bound state.

The factors that explained the modesty of the effects of the complex potential in the weakly-bound ^{11}Be can be used to understand the larger effect on ^{41}Ca. The larger binding energy in ^{41}Ca extends the cross section to larger n-^{40}Ca energies, where the effect of the imaginary potential is larger. In addition, the imaginary potential is larger in the KD interaction, with a surface term that is present even at zero energy, which explains the strong effect even at low energies.

This reduction of the cross section, which is found to be heavily dependent on the binding energy of the removed nucleon, bears a tantalizing resemblance to that found in nucleon-knockout reactions at intermediate energies, where experimental cross sections show a significant reduction when compared to theoretical calculations when removing the deeply-bound species in an asymmetric nucleus, but barely any reduction when removing the weakly-bound species [2,15]. This reduction is a currently heavily-debated topic, since a similar trend was not found for transfer [36] and quasifree proton-induced removal reactions [37–39]. A recent overview on this topic can be found in [40].

It should be noted that the kind of effects explored in this work, that is, the absorption of the valence particle due to the interaction with the core (which may lead to a destruction of the core) are not considered in the usual treatment of high-energy nucleon-knockout reactions, which is usually described in the eikonal sudden approximation [41] in which, during the collision, the core and valence nucleon are assumed to move independently and not interact. On the other hand, both in proton-induced reactions, with the usual description with the Distorted-Wave Impulse Approximation (DWIA) [3,42–44], and in transfer reactions, with the widely-used DWBA, this interaction and possible absorption is considered, at least in an approximate way.

The method presented in this work has been developed for the so-called exclusive or diffractive breakup reactions, in which the valence and core particles survive and are detected. However, in nucleon-knockout reactions, specially for deeply-bound nucleons, the main contributor to the cross section is the stripping reaction, in which the valence particle is absorbed and only the core is detected. This requires a description beyond CDCC, such as the aforementioned eikonal sudden approximation or the quantum IAV model [16,45]. Extensions of these models to include core-valence absorption are, by the results of this work, promising avenues to solve the open problem of the reduction factors in nucleon-removal cross sections and their exploration is currently underway.

4. Summary and conclusions

In this work, we have presented a method for extending the CDCC formalism to include absorption and excitation effects between core and valence particle via the use of complex energy-dependent potentials, which require a binormal basis for discretized continuum states to ensure orthogonality. The method has been applied to study the breakup cross sections for the reactions $^{12}C(^{11}Be, ^{10}Be + n)^{12}C$ and $^{12}C(^{41}Ca, ^{40}Ca + n)^{12}C$ at 70 MeV/A, finding a moderate reduction of the cross section for the breakup of ^{11}Be and a much larger reduction for ^{41}Ca, which is associated to the larger binding energy of the latter. This dependence of the reduction of the cross section on the binding-energy of the removed species is very similar to the open problem of the reduction factors in nucleon-knockout reactions and offers an explanation for these reduction factors in the absorption due to the interaction between valence nucleon and residual core. Further investigation is required on this topic, in particular the extension of these effects to stripping cross sections. The method presented in this work permits the inclusion of open channels in the study of breakup reactions, whose effects are ignored in their usual description. Therefore, it allows for a more realistic treatment of these reactions, in particular in the removal of more deeply-bound nucleons, for which these effects are more important. The effects of absorption on resonant states are found to be particularly intense, for resonances at moderate and high excitation energies, where open channels exist. So, they should be considered for a proper understanding of the relation of the structure properties of these resonances with the measured cross sections. Given that the present method only modifies the coupling potentials, its inclusion in standard nuclear reaction codes such as FRESCO [46] is straightforward. The results of this work also open up the study of breakup reactions with microscopic optical potentials, which up until now were precluded from use in CDCC calculations due to them being complex and energy-dependent. Therefore, the presented formalism serves as a connection between state-of-the-art descriptions of nuclear reactions and nuclear structure.

Declaration of competing interest

The authors declare that they have no known competing financial interests or personal relationships that could have appeared to influence the work reported in this paper.

Acknowledgements

This work is partially supported by the I+D+i project PID2020-114687GB-I00 funded by MCIN/AEI/10.13039/501100011033, by the grant Group FQM-160 funded by the Consejería de Economía,

Conocimiento, Empresas y Universidad, Junta de Andalucía (Spain), and by project P20_01247, funded by the Consejería de Economía, Conocimiento, Empresas y Universidad, Junta de Andalucía (Spain) with funds from "ERDF A way of making Europe". M.G.-R. is supported by the Junta de Andalucía under grant number DOC-01006 in the plan PAIDI 2020, which receives funds from the European Social Fund.

References

[1] M.H. Macfarlane, J.B. French, Stripping reactions and the structure of light and intermediate nuclei, Rev. Mod. Phys. 32 (1960) 567–691, https://doi.org/10.1103/RevModPhys.32.567, https://link.aps.org/doi/10.1103/RevModPhys.32.567.

[2] A. Gade, P. Adrich, D. Bazin, M.D. Bowen, B.A. Brown, C.M. Campbell, J.M. Cook, T. Glasmacher, P.G. Hansen, K. Hosier, S. McDaniel, D. McGlinchery, A. Obertelli, K. Siwek, L.A. Riley, J.A. Tostevin, D. Weisshaar, Reduction of spectroscopic strength: weakly-bound and strongly-bound single-particle states studied using one-nucleon knockout reactions, Phys. Rev. C 77 (2008) 044306, https://doi.org/10.1103/PhysRevC.77.044306, https://link.aps.org/doi/10.1103/PhysRevC.77.044306.

[3] G. Jacob, T.A.J. Maris, Quasi-free scattering and nuclear structure, Rev. Mod. Phys. 38 (1966) 121–142, https://doi.org/10.1103/RevModPhys.38.121, https://link.aps.org/doi/10.1103/RevModPhys.38.121.

[4] L. Lapikás, Quasi-elastic electron scattering off nuclei, Nucl. Phys. A 553 (1993) 297–308, https://doi.org/10.1016/0375-9474(93)90630-G, https://www.sciencedirect.com/science/article/pii/037594749390630G.

[5] R. Chatterjee, R. Shyam, Breakup reactions of light and medium mass neutron drip line nuclei, Prog. Part. Nucl. Phys. 103 (2018) 67–108, https://doi.org/10.1016/j.ppnp.2018.06.001, https://www.sciencedirect.com/science/article/pii/S014664101830053X.

[6] V. Pesudo, M.J.G. Borge, A.M. Moro, J.A. Lay, E. Nácher, J. Gómez-Camacho, O. Tengblad, L. Acosta, M. Alcorta, M.A.G. Alvarez, C. Andreoiu, P.C. Bender, R. Braid, M. Cubero, A. Di Pietro, J.P. Fernández-García, P. Figuera, M. Fisichella, B.R. Fulton, A.B. Garnsworthy, G. Hackman, U. Hager, O.S. Kirsebom, K. Kuhn, M. Lattuada, G. Marquínez-Durán, I. Martel, D. Miller, M. Moukaddam, P.D. O'Malley, A. Perea, M.M. Rajabali, A.M. Sánchez-Benítez, F. Sarazin, V. Scuderi, C.E. Svensson, C. Unsworth, Z.M. Wang, Scattering of the halo nucleus ^{11}Be on ^{197}Au at energies around the Coulomb barrier, Phys. Rev. Lett. 118 (2017) 152502, https://doi.org/10.1103/PhysRevLett.118.152502, https://link.aps.org/doi/10.1103/PhysRevLett.118.152502.

[7] N. Fukuda, T. Nakamura, N. Aoi, N. Imai, M. Ishihara, T. Kobayashi, H. Iwasaki, T. Kubo, A. Mengoni, M. Notani, H. Otsu, H. Sakurai, S. Shimoura, T. Teranishi, Y.X. Watanabe, K. Yoneda, Coulomb and nuclear breakup of a halo nucleus ^{11}Be, Phys. Rev. C 70 (2004) 054606, https://doi.org/10.1103/PhysRevC.70.054606, https://link.aps.org/doi/10.1103/PhysRevC.70.054606.

[8] T. Nakamura, N. Fukuda, T. Kobayashi, N. Aoi, H. Iwasaki, T. Kubo, A. Mengoni, M. Notani, H. Otsu, H. Sakurai, S. Shimoura, T. Teranishi, Y.X. Watanabe, K. Yoneda, M. Ishihara, Coulomb dissociation of ^{19}C and its halo structure, Phys. Rev. Lett. 83 (1999) 1112–1115, https://doi.org/10.1103/PhysRevLett.83.1112, https://link.aps.org/doi/10.1103/PhysRevLett.83.1112.

[9] T. Nakamura, A.M. Vinodkumar, T. Sugimoto, N. Aoi, H. Baba, D. Bazin, N. Fukuda, T. Gomi, H. Hasegawa, N. Imai, M. Ishihara, T. Kobayashi, Y. Kondo, T. Kubo, M. Miura, T. Motobayashi, H. Otsu, A. Saito, H. Sakurai, S. Shimoura, K. Watanabe, Y.X. Watanabe, T. Yakushiji, Y. Yanagisawa, K. Yoneda, Observation of strong low-lying $e1$ strength in the two-neutron halo nucleus ^{11}Li, Phys. Rev. Lett. 96 (2006) 252502, https://doi.org/10.1103/PhysRevLett.96.252502, https://link.aps.org/doi/10.1103/PhysRevLett.96.252502.

[10] G.R. Satchler, Direct Nuclear Reactions, Clarendon Press, Oxford (UK), 1983.

[11] N. Austern, Y. Iseri, M. Kamimura, M. Kawai, G. Rawitscher, M. Yahiro, Continuum-discretized coupled-channels calculations for three-body models of deuteron-nucleus reactions, Phys. Rep. 154 (3) (1987) 125–204, https://doi.org/10.1016/0370-1573(87)90094-9, https://www.sciencedirect.com/science/article/pii/0370157387900949.

[12] A.M. Moro, J.A. Lay, Interplay between valence and core excitation mechanisms in the breakup of halo nuclei, Phys. Rev. Lett. 109 (2012) 232502, https://doi.org/10.1103/PhysRevLett.109.232502, https://link.aps.org/doi/10.1103/PhysRevLett.109.232502.

[13] P. Capel, D. Phillips, H.-W. Hammer, Simulating core excitation in breakup reactions of halo nuclei using an effective three-body force, Phys. Lett. B (2021) 136847, https://doi.org/10.1016/j.physletb.2021.136847.

[14] C. Louchart, A. Obertelli, A. Boudard, F. Flavigny, Nucleon removal from unstable nuclei investigated via intranuclear cascade, Phys. Rev. C 83 (2011) 011601, https://doi.org/10.1103/PhysRevC.83.011601, https://link.aps.org/doi/10.1103/PhysRevC.83.011601.

[15] J.A. Tostevin, A. Gade, Updated systematics of intermediate-energy single-nucleon removal cross sections, Phys. Rev. C 103 (2021) 054610, https://doi.org/10.1103/PhysRevC.103.054610, https://link.aps.org/doi/10.1103/PhysRevC.103.054610.

[16] M. Ichimura, N. Austern, C.M. Vincent, Equivalence of post and prior sum rules for inclusive breakup reactions, Phys. Rev. C 32 (1985) 431–439, https://doi.org/10.1103/PhysRevC.32.431, https://link.aps.org/doi/10.1103/PhysRevC.32.431.

[17] L.D. Faddeev, Scattering theory for a three-particle system, Zh. Eksp. Teor. Fiz. 39 (1960) 1459, Sov. Phys. JETP 12 (1961) 1014.

[18] E. Alt, P. Grassberger, W. Sandhas, Reduction of the three-particle collision problem to multi-channel two-particle Lippmann-Schwinger equations, Nucl. Phys. B 2 (2) (1967) 167–180, https://doi.org/10.1016/0550-3213(67)90016-8, http://www.sciencedirect.com/science/article/pii/0550321367900168.

[19] E. Cravo, R. Crespo, A. Deltuva, Valence neutron-core interaction effects on the breakup of halo nuclei, Phys. Rev. C 87 (2013) 034612, https://doi.org/10.1103/PhysRevC.87.034612, https://link.aps.org/doi/10.1103/PhysRevC.87.034612.

[20] W. Dickhoff, R. Charity, Recent developments for the optical model of nuclei, Prog. Part. Nucl. Phys. 105 (2019) 252–299, https://doi.org/10.1016/j.ppnp.2018.11.002, https://www.sciencedirect.com/science/article/pii/S0146641018300875.

[21] A. Idini, C. Barbieri, P. Navrátil, Ab initio optical potentials and nucleon scattering on medium mass nuclei, Phys. Rev. Lett. 123 (2019) 092501, https://doi.org/10.1103/PhysRevLett.123.092501, https://link.aps.org/doi/10.1103/PhysRevLett.123.092501.

[22] J. Rotureau, P. Danielewicz, G. Hagen, G.R. Jansen, F.M. Nunes, Microscopic optical potentials for calcium isotopes, Phys. Rev. C 98 (2018) 044625, https://doi.org/10.1103/PhysRevC.98.044625, https://link.aps.org/doi/10.1103/PhysRevC.98.044625.

[23] N.C. Summers, et al., Extended continuum discretized coupled channels method: core excitation in the breakup of exotic nuclei, Phys. Rev. C 74 (2006) 014606, https://doi.org/10.1103/PhysRevC.74.014606.

[24] R. de Diego, J.M. Arias, J.A. Lay, A.M. Moro, Continuum-discretized coupled-channels calculations with core excitation, Phys. Rev. C 89 (2014) 064609, https://doi.org/10.1103/PhysRevC.89.064609.

[25] R.G. Newton, Scattering Theory of Waves and Particles, Dover, 1982.

[26] B.H. McKellar, C.M. McKay, Formal scattering theory for energy-dependent potentials, Aust. J. Phys. 36 (1983) 607.

[27] D.C. Brody, Biorthogonal quantum mechanics, J. Phys. A, Math. Theor. 47 (3) (2013) 035305, https://doi.org/10.1088/1751-8113/47/3/035305.

[28] P. Capel, G. Goldstein, D. Baye, Time-dependent analysis of the breakup of ^{11}Be on ^{12}C at 67 MeV/nucleon, Phys. Rev. C 70 (2004) 064605, https://doi.org/10.1103/PhysRevC.70.064605, https://link.aps.org/doi/10.1103/PhysRevC.70.064605.

[29] A. Bonaccorso, R.J. Charity, Optical potential for the n-^{9}Be reaction, Phys. Rev. C 89 (2014) 024619, https://doi.org/10.1103/PhysRevC.89.024619, https://link.aps.org/doi/10.1103/PhysRevC.89.024619.

[30] A. Moro, J. Lay, J. Gómez Camacho, Determining B(E1) distributions of weakly bound nuclei from breakup cross sections using continuum discretized coupled channels calculations. Application to ^{11}Be, Phys. Lett. B 811 (2020) 135959, https://doi.org/10.1016/j.physletb.2020.135959, https://www.sciencedirect.com/science/article/pii/S0370269320307620.

[31] T. Furumoto, W. Horiuchi, M. Takashina, Y. Yamamoto, Y. Sakuragi, Global optical potential for nucleus-nucleus systems from 50 MeV/u to 400 MeV/u, Phys. Rev. C 85 (2012) 044607, https://doi.org/10.1103/PhysRevC.85.044607, https://link.aps.org/doi/10.1103/PhysRevC.85.044607.

[32] A. Koning, J. Delaroche, Local and global nucleon optical models from 1 keV to 200 MeV, Nucl. Phys. A 713 (3) (2003) 231–310, https://doi.org/10.1016/S0375-9474(02)01321-0, https://www.sciencedirect.com/science/article/pii/S0375947402013210.

[33] J.A. Lay, A.M. Moro, J.M. Arias, J. Gómez-Camacho, Exploring continuum structures with a pseudo-state basis, Phys. Rev. C 82 (2010) 024605, https://doi.org/10.1103/PhysRevC.82.024605, https://link.aps.org/doi/10.1103/PhysRevC.82.024605.

[34] D.J. Howell, J.A. Tostevin, J.S. Al-Khalili, Coupled channels calculations of ^{11}Be breakup, J. Phys. G, Nucl. Part. Phys. 31 (10) (2005) S1881–S1884, https://doi.org/10.1088/0954-3899/31/10/093.

[35] L.C. Chamon, D. Pereira, M.S. Hussein, M.A. Cândido Ribeiro, D. Galetti, Nonlocal description of the nucleus-nucleus interaction, Phys. Rev. Lett. 79 (1997) 5218–5221, https://doi.org/10.1103/PhysRevLett.79.5218, https://link.aps.org/doi/10.1103/PhysRevLett.79.5218.

[36] F. Flavigny, et al., Limited asymmetry dependence of correlations from single nucleon transfer, Phys. Rev. Lett. 110 (2013) 122503, https://doi.org/10.1103/PhysRevLett.110.122503, https://link.aps.org/doi/10.1103/PhysRevLett.110.122503.

[37] L. Atar, et al., Quasifree $(p,2p)$ reactions on oxygen isotopes: observation of isospin independence of the reduced single-particle strength, Phys. Rev. Lett. 120 (2018) 052501, https://doi.org/10.1103/PhysRevLett.120.052501, https://link.aps.org/doi/10.1103/PhysRevLett.120.052501.

[38] M. Holl, et al., Quasi-free neutron and proton knockout reactions from light nuclei in a wide neutron-to-proton asymmetry range, Phys. Lett. B 795 (2019) 682–688, https://doi.org/10.1016/j.physletb.2019.06.069, https://www.sciencedirect.com/science/article/pii/S0370269319304666.

[39] M. Gómez-Ramos, A. Moro, Binding-energy independence of reduced spectroscopic strengths derived from $(p,2p)$ and (p,pn) reactions with nitrogen and oxygen isotopes, Phys. Lett. B 785 (2018) 511–516, https://doi.org/10.

1016/j.physletb.2018.08.058, https://www.sciencedirect.com/science/article/pii/S0370269318306749.

[40] T. Aumann, C. Barbieri, D. Bazin, C. Bertulani, A. Bonaccorso, W. Dickhoff, A. Gade, M. Gómez-Ramos, B. Kay, A. Moro, T. Nakamura, A. Obertelli, K. Ogata, S. Paschalis, T. Uesaka, Quenching of single-particle strength from direct reactions with stable and rare-isotope beams, Prog. Part. Nucl. Phys. 118 (2021) 103847, https://doi.org/10.1016/j.ppnp.2021.103847, https://www.sciencedirect.com/science/article/pii/S0146641021000016.

[41] P. Hansen, J. Tostevin, Direct reactions with exotic nuclei, Annu. Rev. Nucl. Part. Sci. 53 (1) (2003) 219–261, https://doi.org/10.1146/annurev.nucl.53.041002.110406.

[42] G. Jacob, T.A.J. Maris, Quasi-free scattering and nuclear structure. II, Rev. Mod. Phys. 45 (1973) 6–21, https://doi.org/10.1103/RevModPhys.45.6, https://link.aps.org/doi/10.1103/RevModPhys.45.6.

[43] K. Ogata, K. Yoshida, K. Minomo, Asymmetry of the parallel momentum distribution of (p, pn) reaction residues, Phys. Rev. C 92 (2015) 034616, https://doi.org/10.1103/PhysRevC.92.034616, https://link.aps.org/doi/10.1103/PhysRevC.92.034616.

[44] T. Aumann, C.A. Bertulani, J. Ryckebusch, Quasifree $(p,2p)$ and (p,pn) reactions with unstable nuclei, Phys. Rev. C 88 (2013) 064610, https://doi.org/10.1103/PhysRevC.88.064610, https://link.aps.org/doi/10.1103/PhysRevC.88.064610.

[45] J. Lei, A.M. Moro, Reexamining closed-form formulae for inclusive breakup: application to deuteron- and ^{6}Li-induced reactions, Phys. Rev. C 92 (2015) 044616, https://doi.org/10.1103/PhysRevC.92.044616, https://link.aps.org/doi/10.1103/PhysRevC.92.044616.

[46] I.J. Thompson, Coupled reaction channels calculations in nuclear physics, Comput. Phys. Rep. 7 (4) (1988) 167–212, https://doi.org/10.1016/0167-7977(88)90005-6, https://www.sciencedirect.com/science/article/pii/0167797788900056.